JOURNAL OF SOLID STATE CHEMISTRY 66, 40–46 (1987)

Structure Determination of Low-Dimensional Conductor Mo_8O_{23}

H. FUJISHITA, M. SATO,* S. SATO, AND S. HOSHINO

Institute for Solid State Physics, University of Tokyo, Roppongi, Minato-ku, Tokyo 106, Japan

Received December 3, 1985; in revised form April 14, 1986

The crystal structure of the new low-dimensional conductor Mo_8O_{23} has been determined at 370 and 100 K using a four-circle X-ray diffractometer. Mo_8O_{23} has an incommensurate structure at room temperature and the incommensurate–commensurate phase transition takes place at about 285 K. The structure of the normal phase at 370 K is essentially the same as that presented by Magnéli for room temperature. The structure of commensurate phase at 100 K can be described mainly by the inhomogeneous rotations of MoO_6 octahedra. © 1987 Academic Press, Inc.

Introduction

Compound series of transition metal oxides TO_{n-x} and so-called bronzes M_xTO_n have recently attracted much attention (*1*). The crystal structures of these compounds are characterized by a linkage of TO_6 octahedra. These compounds often show low-dimensional conductivity due to the anisotropic overlap of wavefunctions of electrons caused by a small anisotropy of the linkage. In the case of molybdenum bronzes, $K_{0.3}MoO_3$ is a quasi-one-dimensional conductor (*2*), though it seems to have the two-dimensional structure; on the other hand, $K_{0.9}Mo_6O_{17}$ is a quasi-two-dimensional conductor (*3*). In this report the structure of the new low-dimensional conductor Mo_8O_{23} (i.e., $MoO_{3-0.125}$) at 370 and 100 K are described in detail.

Recently we reported the anomalies in electrical resistivities and magnetic susceptibility in Mo_8O_{23} (*4*). The structure seems to have a two-dimensional character at first sight. However, the temperature dependence of the ratios of resistivities along three orthogonal directions suggested that Mo_8O_{23} was a quasi-one-dimensional conductor at high temperatures and had a two-dimensional character with the formation of a charge density wave (CDW) in the low-temperature region. The temperature dependence of the magnetic susceptibility also suggested that the anomalous behavior of the resistivity was caused by the CDW in the quasi-one-dimensional conductor.

Other evidence of the CDW state is given by X-ray and neutron diffraction studies (*1*). Superlattice reflections with the incommensurate wave vector $\bar{q}_{inc} \simeq (0.195, 0.5, 0.120)$ can be seen at room temperature. The incommensurate CDW undergoes the lock-in transition at $T_{c2} \simeq 285$ K and the wave vector of the superlattice reflections suddenly becomes $\bar{q} = (0.0, 0.5, 0.0)$. The width of the superlattice peak is almost

* Present address: Institute for Molecular Science, 38 Nishigonaka, Myodaiji, Okazaki 444, Japan.

0022-4596/87 $3.00

equal to that of the fundamental one, indicating that both the incommensurate and the commensurate CDW have the long range order. The normal–incommensurate phase transition is deduced to take place at $T_{c1} \lesssim 360$ K from the temperature dependence of the intensity of superlattice reflections, though the precise value of T_{c1} has not been obtained.

The room-temperature structure of Mo_8O_{23} had been presented by Magnéli (*5*). The crystal has a monoclinic structure with a space group $P2/c-C_{2h}^4$ (No. 13). The structure is made up of a combination of MoO_6 octahedra: They link up at their corners or edges to each other. The atomic coordinates at room temperature are not accurate because the structure is known to be incommensurate.

The crystal structure analysis of Mo_8O_{23} at 370 and 100 K has been carried out to clarify the feature of the CDW state. There is no serious difference between the structure presented by Magnéli and the high-temperature structure. The low-temperature structure can be described mainly by inhomogeneous rotations of MoO_6 octahedra associated with a M_3 mode of the ReO_3-type cubic lattice.

Experimental

The single crystals of Mo_8O_{23} were obtained by the method described by Magnéli (*5*). A sample crystal used for X-ray diffraction was shaped to a sphere with a radius of 0.15 mm ($\mu r = 0.8$ for Mo$K\alpha$).

X-Ray diffraction intensities were collected on a Rigaku automated four-circle diffractometer. Mo$K\alpha$ radiation was used. Reflections with $2\theta \leq 55°$ were measured. Cu$K\alpha$ radiation was also used to check multiple reflections. Measurements were made at 370 and 100 K. The sample crystal was cooled and heated by a regulated nitrogen vapor stream and a hot air one, respectively. Conventional absorption, Lp, and extinction corrections were made for diffraction intensities. The structures were refined by the least-square method. All computations were carried out on a FACOM M-360 computer at ISSP.

Results and Discussions

(a) Structure at 370 K

Diffraction data at 370 K were analyzed using the monoclinic space group $P2/c-C_{2h}^4$ (No. 13), which was presented for room-temperature structure by Magnéli (*5*). The incommensurate super-lattice reflections disappear at 370 K, which justifies the adoption of the space group. The crystal data are $a = 13.384(3)$ Å, $b = 4.0616(5)$ Å, $c = 16.883(3)$ Å, $\beta = 106.27(2)°$, $Z = 2$. The numbers of the reflection data ($|F_0| > 3\sigma(|F_0|)$) and the parameters are 1972 and 143, respectively. The discrepancy index R is 0.0271. The final atomic coordinates and the anisotropic thermal parameters are listed in Table I. The isotropic extinction parameter is $0.150(4) \times 10^{-4}$. There is no serious difference between the present structure and that presented by Magnéli, especially for Mo atoms.

The unit cell contains four crystallographically independent Mo sites. Each Mo atom is surrounded by six oxygen atoms; they form a distorted MoO_6 octahedron. The octahedra form the ReO_3-type crystal sheets in the *bc* plane as shown in Fig. 1a by the linkage of the corners of the octahedra. There are clusters made of four edge-sharing MoO_6 octahedra in the *ac* plane as shown in Fig. 1b. The crystal sheets are connected by the chains of the clusters. The existence of the edge-linked clusters of MoO_6 octahedra causes the oxygen deficiencies, which donate the conduction electrons. The projection of the structure on the *ac* plane is shown in Fig. 2.

It may be helpful to note that there are three kinds of octahedra as regards the con-

TABLE I

FRACTIONAL COORDINATES AND THERMAL PARAMETERS OF ATOMS IN Mo_8O_{23} AT 370 K

	x	y	z	U_{11}	U_{22}	U_{33}	U_{12}	U_{13}	U_{23}
Mo_1	0.06397(4)	0.5850(2)	0.41655(3)	0.0069(2)	0.0078(3)	0.0071(3)	0.0000(3)	0.0017(2)	−0.0001(3)
Mo_2	0.18514(4)	0.4131(2)	0.24568(3)	0.0063(2)	0.0080(3)	0.0071(3)	−0.0006(3)	0.0013(2)	0.0001(3)
Mo_3	0.31501(4)	0.5900(2)	0.07903(3)	0.0060(3)	0.0079(3)	0.0076(3)	−0.0002(3)	0.0015(2)	−0.0002(3)
Mo_4	0.44659(4)	0.4079(2)	0.40204(3)	0.0056(2)	0.0079(3)	0.0070(3)	0.0000(3)	0.0004(2)	−0.0007(3)
O_1	0.0658(4)	−0.0012(10)	0.4164(3)	0.025(3)	0.010(3)	0.029(3)	0.002(2)	−0.001(2)	0.000(2)
O_2	0.1911(4)	0.9971(9)	0.2458(3)	0.025(3)	0.009(3)	0.027(3)	0.000(2)	0.001(3)	0.000(2)
O_3	0.3191(4)	0.0069(10)	0.0770(3)	0.017(3)	0.013(3)	0.028(3)	0.000(2)	0.004(2)	−0.001(2)
O_4	0.4469(4)	0.9918(9)	0.4074(3)	0.014(3)	0.009(3)	0.023(3)	−0.001(2)	0.005(2)	−0.002(2)
O_5	0.0	0.5	0.0	0.013(3)	0.026(5)	0.010(3)	0.001(3)	0.009(3)	−0.001(3)
O_6	0.0645(4)	0.4943(10)	0.1643(3)	0.010(2)	0.022(3)	0.012(2)	−0.001(2)	−0.002(2)	−0.001(2)
O_7	0.1293(3)	0.4930(10)	0.3303(3)	0.013(2)	0.031(4)	0.010(2)	−0.002(2)	0.006(2)	−0.002(2)
O_8	0.1989(3)	0.4945(10)	0.4960(3)	0.011(3)	0.022(4)	0.012(3)	0.001(2)	−0.001(2)	0.001(2)
O_9	0.2612(3)	0.5144(10)	0.1632(3)	0.010(2)	0.030(4)	0.010(2)	0.003(2)	0.004(2)	0.003(2)
O_{10}	0.3261(3)	0.4891(10)	0.3282(3)	0.015(3)	0.020(3)	0.014(3)	−0.002(2)	0.002(2)	−0.001(2)
O_{11}	0.4113(3)	0.5015(9)	0.0045(3)	0.009(2)	0.012(3)	0.006(2)	0.000(2)	0.004(2)	0.000(2)
O_{12}	0.4570(3)	0.4908(10)	0.1532(3)	0.009(2)	0.019(3)	0.004(2)	−0.001(2)	0.000(2)	0.001(2)

Note. The space group is $P2/c$. The anisotropic thermal parameters U_{ij}, are defined by $\exp[-2\pi^2U_{11}h^2a^{*2} + U_{22}k^2b^{*2} + U_{33}l^2c^{*2} + 2U_{12}hka^*b^* + 2U_{13}hla^*c^* + 2U_{23}klb^*c^*)]$ and are given in Å^2.

nection with other MoO_6 octahedra in the ac plane: (a) The octahedra share their corners with four other octahedra. (b) The octahedra share their corners with two other octahedra and an edge with another one. (c) The octahedra share a corner and two edges with other octahedra.

(b) Structure at 100 K

Mo_8O_{23} exhibits a lock-in transition at $T_{c2} \simeq 285$ K. Superlattice reflections appear at $\bar{q} = (0.0, 0.5, 0.0)$ below T_{c2}. This fact indicates that the lattice parameter b is twice as long as that of the highest temperature phase. The crystal data are $a = 13.39(1)$ Å, $b = 8.062(3)$ Å, $c = 16.82(1)$ Å, $\beta = 106.02(6)°$, $Z = 4$. Several weak reflections which indicate the disappearance of the c-glide plane have been observed. To examine whether or not they are caused by multiple reflections, the integrated intensities were measured by rotating the sample around the scattering vectors. Though the reflections did not disappear by the rotation, the intensities changed very rapidly: The intensities made peaks almost every 2° rotation and no flat regions of the intensities were detected.

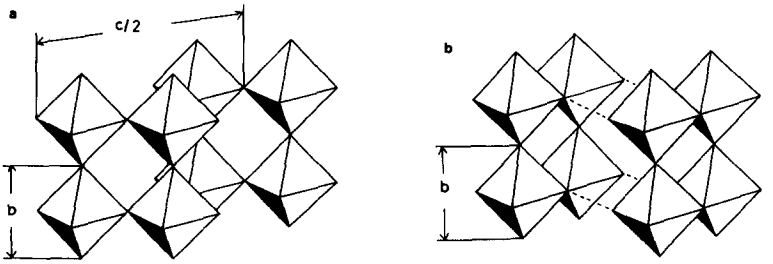

FIG. 1. (a) The ReO_3-type crystal sheet in the bc plane is shown schematically. It is made of the linkage of the corners of MoO_6 octahedra. (b) The cluster formed by the four MoO_6 octahedra in the ac plane is shown schematically. It is made of the linkage of the edges of MoO_6 octahedra.

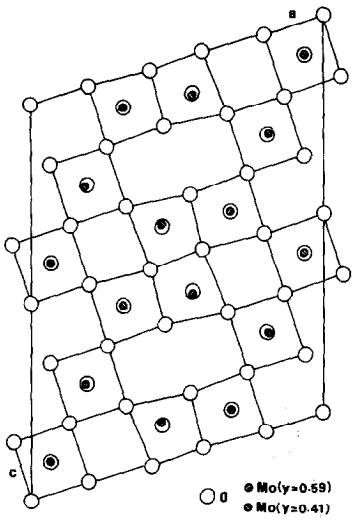

FIG. 2. The projection of the structure of Mo_8O_{23} at 370 K on the *ac* plane. The unit cell contains one layer of MoO_6 octahedra perpendicular to the *b* axis.

Thus it is very plausible that the reflections are due to multiple reflections, which leads the space group to any of Pc, $P2/c$ and $P2_1/c$: $P2_1/c$ is included because of the doubling of the unit cell along *b*. Calculations showed that the space groups $P2/c$ and $P2_1/c$ should be excluded because of the large discrepancy indices *R*.

Detailed analysis was made using the space group $Pc-C_s^2$ (No. 7). The isotropic thermal parameters are adopted for Mo atoms. Those for oxygen atoms are fixed at about $\frac{1}{4}$ of the corresponding values at 370 K. These assumptions are adopted to decrease the number of parameters of the refinement. The number of the reflection data ($|F_0| > 3\sigma(|F_0|)$) is 2442 (1737 and 705 for fundamental reflections and superlattice ones, respectively). The number of the parameters refined is 202. The discrepancy index *R* is 0.0358. The atomic coordinates and the thermal parameters are listed in Table II. In this table the origin of coordinates

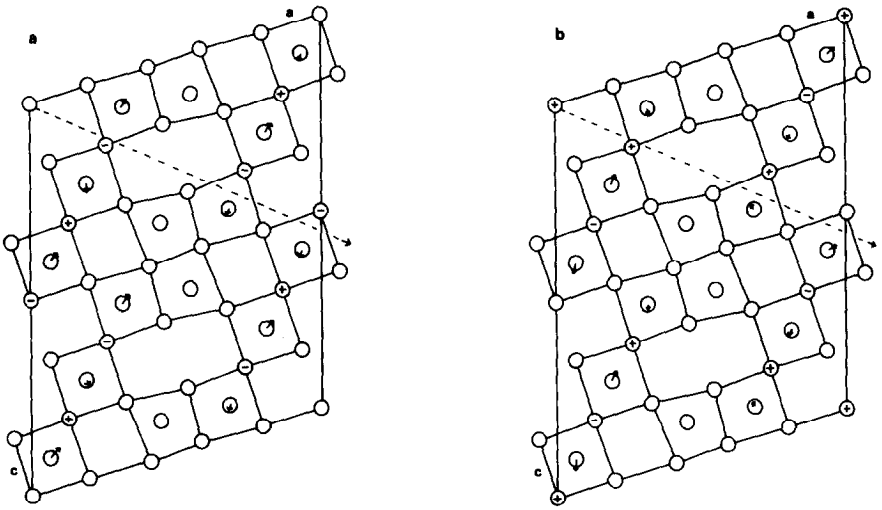

FIG. 3. The projection of the structure of Mo_8O_{23} at 100 K on the *ac* plane. (a) Lower and (b) upper halves are shown separately. The unit cell contains two layers of MoO_6 octahedra perpendicular to the *b* axis. Mo atoms are omitted because they suffer almost no shifts. The arrows and + or − signs denote the directions of displacements of oxygen atoms; only the large displacements are indicated. The length of the arrow shows the relative displacement only qualitatively. Arrows delineated by broken lines indicate the direction of the incommensurate wave vector $\bar{q}_{inc}$ in the *ac* plane.

TABLE II

FRACTIONAL COORDINATES AND THERMAL PARAMETERS OF ATOMS IN Mo_8O_{23} AT 100 K

	x	y	z	B
Mo_{11}	0.0612(20)	0.2916(3)	0.4188(12)	0.19(5)
Mo_{12}	0.9348(20)	0.2923(4)	0.0817(12)	0.24(5)
Mo_{13}	0.0649(20)	0.7928(3)	0.4170(12)	0.25(5)
Mo_{14}	0.9325(20)	0.7935(3)	0.0847(12)	0.24(5)
Mo_{21}	0.1842(20)	0.2087(3)	0.2479(12)	0.13(5)
Mo_{22}	0.8176(20)	0.2060(3)	0.2543(12)	0.33(5)
Mo_{23}	0.1862(20)	0.7070(3)	0.2448(12)	0.22(5)
Mo_{24}	0.8156(20)	0.7049(3)	0.2563(12)	0.29(5)
Mo_{31}	0.3154(20)	0.2899(3)	0.0796(12)	0.12(5)
Mo_{32}	0.6851(20)	0.2954(3)	0.4187(12)	0.37(5)
Mo_{33}	0.3156(20)	0.7936(3)	0.0774(12)	0.16(5)
Mo_{34}	0.6845(20)	0.7997(3)	0.4210(12)	0.31(5)
Mo_{41}	0.4472(20)	0.2043(3)	0.4015(12)	0.25(4)
Mo_{42}	0.5537(20)	0.2060(3)	0.0970(12)	0.23(4)
Mo_{43}	0.4470(20)	0.7036(3)	0.4012(12)	0.27(4)
Mo_{44}	0.5546(20)	0.7049(3)	0.0981(12)	0.23(4)
O_{11}	0.0779(24)	−0.0011(25)	0.4050(17)	0.5
O_{12}	0.9272(24)	0.0012(29)	0.0891(17)	0.5
O_{13}	0.0607(23)	0.4990(27)	0.4296(16)	0.5
O_{14}	0.9514(23)	0.5048(27)	0.0783(16)	0.5
O_{21}	0.1929(23)	0.4912(25)	0.2339(16)	0.5
O_{22}	0.7976(23)	0.5040(26)	0.2613(16)	0.5
O_{23}	0.1900(23)	0.9971(28)	0.2574(16)	0.5
O_{24}	0.8216(23)	0.9960(27)	0.2478(17)	0.5
O_{31}	0.3214(24)	0.0082(31)	0.0670(17)	0.4
O_{32}	0.6813(24)	0.0060(31)	0.4303(18)	0.4
O_{33}	0.3152(23)	0.5000(30)	0.0882(16)	0.4
O_{34}	0.6775(23)	0.5067(29)	0.4152(16)	0.4
O_{41}	0.4436(23)	0.4978(24)	0.4074(16)	0.25
O_{42}	0.5460(23)	0.4885(22)	0.0995(15)	0.25
O_{43}	0.4521(23)	0.9891(22)	0.4152(15)	0.25
O_{44}	0.5580(24)	0.9974(24)	0.0935(15)	0.25
O_{51}	−0.0002	0.2505(15)	−0.0015	0.2
O_{52}	0.0024(20)	0.7900(15)	−0.0015(12)	0.2
O_{61}	0.0606(24)	0.2467(35)	0.1601(16)	0.3
O_{62}	0.9328(23)	0.2429(32)	0.3282(15)	0.3
O_{63}	0.0601(23)	0.7542(31)	0.1589(16)	0.3
O_{64}	0.9327(23)	0.7428(34)	0.3317(17)	0.3
O_{71}	0.1265(19)	0.2707(25)	0.3274(14)	0.25
O_{72}	0.8668(25)	0.2776(25)	0.1659(17)	0.25
O_{73}	0.1341(23)	0.7186(26)	0.3288(17)	0.25
O_{74}	0.8756(19)	0.7193(23)	0.1692(15)	0.25
O_{81}	0.2011(22)	0.2464(35)	0.4929(15)	0.3
O_{82}	0.8006(23)	0.2582(29)	−0.0010(16)	0.3
O_{83}	0.1943(24)	0.7351(25)	0.4921(16)	0.3
O_{84}	0.7994(23)	0.7476(34)	0.0018(17)	0.3
O_{91}	0.2593(21)	0.2437(27)	0.1578(14)	0.25
O_{92}	0.7417(21)	0.2290(23)	0.3336(15)	0.25
O_{93}	0.2579(24)	0.7718(24)	0.1605(17)	0.25
O_{94}	0.7351(22)	0.7823(23)	0.3300(15)	0.25

TABLE II—*Continued*

	x	*y*	*z*	*B*
O_{101}	0.3226(27)	0.2545(29)	0.3243(16)	0.25
O_{102}	0.6708(25)	0.2316(22)	0.1706(16)	0.25
O_{103}	0.3225(24)	0.7445(30)	0.3215(15)	0.25
O_{104}	0.6702(23)	0.7512(32)	0.1657(15)	0.25
O_{111}	0.4085(26)	0.2580(32)	0.0033(16)	0.15
O_{112}	0.5842(24)	0.2620(29)	0.4930(16)	0.15
O_{113}	0.4024(23)	0.7451(29)	−0.0013(15)	0.15
O_{114}	0.5864(25)	0.7398(28)	0.4904(15)	0.15
O_{121}	0.4542(24)	0.2477(28)	0.1492(15)	0.15
O_{122}	0.5416(26)	0.2337(25)	0.3391(16)	0.15
O_{123}	0.4514(26)	0.7444(28)	0.1512(16)	0.15
O_{124}	0.5319(24)	0.7539(27)	0.3435(17)	0.15

Note. The space group is *Pc*. The origin in the *xz* plane is chosen so as to fix the center of gravity of Mo atoms at the same position as that for 370 K. The isotropic thermal parameter B is defined by $\exp[-B(\sin\theta/\lambda)^2]$ and given in Å^2. The unit cell contains two layers of MoO_6 octahedra perpendicular to the *b* axis.

in the *xz* plane is chosen so as to fix the center of gravity of Mo atoms at the same position as that of the highest temperature phase. The isotropic extinction parameter is $0.143(14) \times 10^{-4}$.

Mo atoms are found to suffer almost no shifts about the origin. The displacements of oxygen atoms from the highest temperature phase are shown in Fig. 3; only the large displacements are indicated. The direction of the incommensurate wave vector $\bar{q}_{inc}$ in the *ac* plane is delineated by a broken line. The direction is nearly parallel to the linkage of the corners of MoO_6 octahedra. The crystal structure of Mo_8O_{23} consists mainly of a ReO_3-type cubic lattice which is shown in Fig. 1a; the intensity distribution of the fundamental reflections indicates the feature of the ReO_3-type cubic lattice. The intensities of superlattice reflections are strong at the point near the "*M* points" of the ReO_3-type "cubic" reciprocal lattice. The intensity distribution of superlattice reflections on the plane with half integer *k* suggests the transverse displacements of atoms about the wave vector of the incommensurate phase: The intensities are weak at the reciprocal lattice points around the direction of $\bar{q}_{inc}$ in the plane and they are strong at the points around the direction perpendicular to $\bar{q}_{inc}$ in the plane. From these facts, the displacements are expected to have a character somewhat similar to that of an M_3 mode in the ReO_3-type cubic lattice: The displacements associated with the M_3 mode are described by the antiphase rotations of neighboring octahedra around some axis and the in-phase rotations of neighboring octahedra along the axis while keeping the corner-linked structure. In fact, the actual shifts of oxygen atoms are mainly described by the rotations of MoO_6 octahedra around the incommensurate wave vector $\bar{q}_{inc}$ in the *ac* plane, though the rotations are not homogeneous and are accompanied by the distortion of octahedra.

In summary, structure analysis of Mo_8O_{23} was made at high and low temperatures. We could refine the high-temperature struc-

ture. The displacements of atoms were obtained in the lowest temperature phase with the commensurate CDW.

References

1. M. SATO, H. FUJISHITA, S. SATO, AND S. HOSHINO. *J. Phys. C* **19,** 3059 (1986).
2. G. TRAVAGLINI, P. WACHTER, J. MARCUS, AND C. SCHLENKER, *Solid State Commun.* **37,** 599 (1981).
3. H. VINCENT, M. GHEDIRA, J. MARCUS, J. MERCIER, AND C. SCHLENKER, *J. Solid State Chem.* **47,** 113 (1983).
4. M. SATO, K. NAKAO, AND S. HOSHINO, *J. Phys. C* **17,** L817 (1984).
5. A. MAGNÉLI, *Acta Chem. Scand.* **2,** 501 (1948).